Progress in Earth
and Planetary Science
a SpringerOpen Journal

RESEARCH ARTICLE

Open Access

CrossMark

Complex inner core boundary from frequency characteristics of the reflection coefficients of PKiKP waves observed by Hi-net

Satoru Tanaka[1*] and Hrvoje Tkalčić[2]

Abstract

Frequency-dependent reflection coefficients of P waves at the inner core boundary (ICB) are estimated from the spectral ratios of PKiKP and PcP waves observed by the high-sensitivity seismograph network (Hi-net) in Japan. The corresponding PKiKP reflection locations at the ICB are distributed beneath the western Pacific. At frequencies where noise levels are sufficiently low, spectra of reflection coefficients show four distinct sets of characteristics: a flat spectrum, a spectrum with a significant spectral hole at approximately 1 or 3 Hz, a spectrum with a strong peak at approximately 2 or 3 Hz, and a spectrum containing both a sharp peak and a significant hole. The variety in observed spectra suggests complex lateral variations in ICB properties. To explain the measured differences in frequency characteristics of ICB reflection coefficients, we conduct 2D finite difference simulations of seismic wavefields near the ICB. The models tested in our simulations include a liquid layer and a solid layer above the ICB, as well as sinusoidal and spike-shaped ICB topography with varying heights and scale lengths. We find that the existence of a layer above the ICB can be excluded as a possible explanation for the observed spectra. Furthermore, we find that an ICB topographic model with wavelengths and heights of several kilometers is too extreme to explain our measurements. However, restricting the ICB topography to wavelengths and heights of 1.0–1.5 km can explain the observed frequency-related phenomena. The existence of laterally varying topography may be a sign of lateral variations in inner core solidification.

Keywords: Inner core boundary; Topography; PKiKP; Finite difference modeling
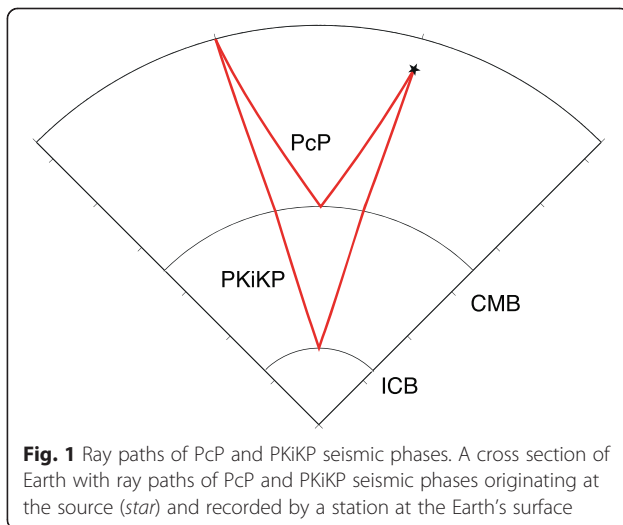
Background

The inner core boundary (ICB) is one of the vital regions for understanding the Earth's core dynamics (Loper and Roberts 1981; Loper 1983; Bergman and Fearn 1994; Shimizu et al. 2005; Deguen et al. 2007; Sumita and Bergman 2009; Deguen 2012). Seismological studies of the ICB and its inferred characteristics, such as the density jump between the inner and the outer cores, the shear-wave velocity at the top of the inner core, and scattering of seismic energy from small-scale topography at the inner core surface, are important in elucidating the growth mechanism of the inner core and the source of the geodynamo (Souriau 2007; Sumita and Bergman 2009; Deuss 2014; Tkalčić 2015).

The hypothesis of a hemispherical structure in the upper inner core (Tanaka and Hamaguchi 1997) has been widely accepted because it is supported by seismic observations of body waves and free oscillations (Creager 1999; Deuss et al. 2010). Hemispherical dichotomy is recognized as a global phenomenon near the ICB (Niu and Wen 2001; Waszek et al. 2011) and possibly near the center of the inner core (Lythgoe et al. 2014). To explain the hemispherical structure of the inner core, two models have been proposed: a large-scale asymmetric flow in the outer core (Sumita and Olson 1999; Aubert et al. 2008; Gubbins et al. 2011) and translational convection in the inner core (Alboussiere et al. 2010; Monnereau et al. 2010). The nature of these models is that they allow diametrically opposite scenarios of freezing and melting, i.e., one of the two hemispheres solidifies faster than the other. This has raised further questions about whether the surface of the inner core in

* Correspondence: stan@jamstec.go.jp
[1]Department of Deep Earth Structure and Dynamics Research, Japan Agency for Marine-Earth Science and Technology, Yokosuka 237-0061, Japan
Full list of author information is available at the end of the article

Springer

Fig. 1 Ray paths of PcP and PKiKP seismic phases. A cross section of Earth with ray paths of PcP and PKiKP seismic phases originating at the source (*star*) and recorded by a station at the Earth's surface

the eastern hemisphere is melting or freezing. Although translational convection models predict that the eastern hemisphere is melting, outer-core large asymmetric flow models disagree about which hemisphere is melting, due to the problem setting, e.g., heat flux at the core–mantle boundary (CMB) and outer core dynamics.

Measurements of PKiKP/PcP amplitude ratios have been used to infer the density jump at the ICB, as well as to determine the shear velocity at the top of the inner core. A sketch of their ray paths is shown in Fig. 1. Studies in the twentieth century usually analyzed PKiKP recorded on short-period seismographs with a predominant frequency of 1 Hz (Engdahl et al. 1970; Buchbinder 1972; Engdahl et al. 1974; Souriau and Souriau 1989; Shearer and Masters 1990). These pioneering studies may have been hampered by the small number of observations and the large scatter in PKiKP/PcP amplitude ratios due to the nature of noisy amplitude measurements (Tkalčić et al. 2009). Another factor influencing the amplitude ratios, and possibly the anticorrelation between the two phases, is the occurrence of near-receiver crustal and mantle heterogeneity (Tkalčić et al. 2010).

The new era of modern instruments, dense networks, and improved global coverage enables observation of a large number of PKiKP and PcP phases on the same seismogram. For example, Koper et al. (2003) analyzed a significant number of PKiKP phases at shorter distances recorded by small aperture arrays of the International Monitoring System. This study was followed by a large number of new studies (Cao and Romanowicz 2004; Koper et al. 2004; Koper and Pyle 2004; Poupinet and Kennett 2004; Koper and Dombrovskaya 2005; Krasnoshchekov et al. 2005; Leyton et al. 2005; Kawakatsu 2006; Leyton and Koper 2007a, b; Peng et al. 2008).

More specifically, Koper and Pyle (2004) measured PKiKP/PcP amplitude ratios from seismograms filtered between 1 and 3 Hz. Their analysis did not reveal any differences between the eastern and western hemispheres of the inner core. Using phases from a Mariana event observed in Japan, whose raypaths sampled the ICB beneath the western Pacific, Kawakatsu (2006) found little scattering energy in the PKiKP coda. However, Leyton and Koper (2007b) analyzed the coda of PKiKP and suggested the existence of small-scale heterogeneities in the uppermost inner core. This result indicates that the strong scattering region is located beneath the Pacific Ocean and Asia, which covers parts of the eastern and western hemispheres. On the basis of scattering properties and Q structure, Cormier (2007) inferred textural differences between the eastern and western hemispheres near the surface of the inner core, including vertically oriented structures in the eastern hemisphere.

Interestingly, the existence of a high-frequency PKiKP phase (up to 5 Hz) with steep incidence angles at the ICB was first observed by Poupinet and Kennett (2004) using phases recorded by narrow-aperture arrays and temporal broadband networks on the Australian continent, whose reflection points were in the eastern hemisphere. Recently, the same class of PKiKP waves was observed in the eastern hemisphere on Chinese and Japanese short-period and broadband stations (J-array) (Tkalčić et al., 2009, 2010) and by the high-sensitivity seismograph network (Hi-net) in Japan (Dai et al. 2012, Jiang and Zhao 2012).
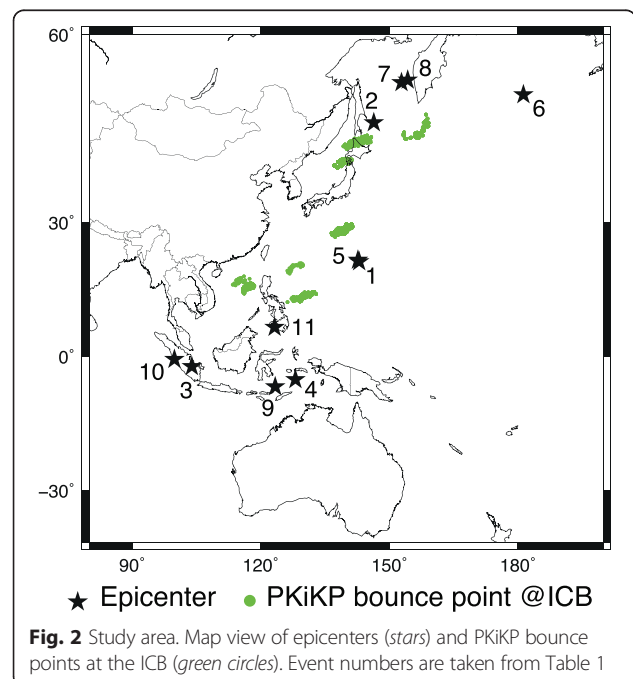

Fig. 2 Study area. Map view of epicenters (*stars*) and PKiKP bounce points at the ICB (*green circles*). Event numbers are taken from Table 1

Table 1 Event list

Event	Date	Time (UTC)	Lat. (°)	Lon. (°)	Depth (km)	m_b	Remarks	No. of used records
1	20010703	13:10:42.60	21.641	142.984	290.0	6.0	DC	73
2	20021117	04:53:48.46	47.946	146.419	470.2	5.8	Sm	58
3	20040725	14:35:19.06	−2.427	103.981	582.1	6.8	DC	83
4	20060127	16:58:53.67	−5.473	128.131	397.0	7.0	Sm	77
5	20070928	13:38:57.88	22.013	142.668	260.0	6.7	Sm	41
6	20080322	21:24:11.27	52.176	−178.716	132.0	5.8	Sm	65
7	20080705	02:12:04.48	53.882	152.886	632.8	6.8	DC	49
8	20081124	09:02:58.76	54.203	154.322	492.3	6.5	DC	83
9	20090828	01:51:20.40	−7.146	123.427	642.4	6.3	DC	31
10	20090930	10:16:09.25	−0.720	99.867	81.0	7.1	DC	33
11	20100723	23:15:10.19	6.780	123.260	640.0	7.4	Sm	53

Hypocenters are taken from the Earthquake data report provided by U.S.G.S.
DC double couple, *Sm* smoothed radiation pattern

To contribute to a better understanding of inner core dynamics and to constrain ICB structure in the eastern hemisphere, here, we collect an extensive dataset of PKiKP waves recorded by Hi-net in Japan. Our aim is to shift focus from analyzing a single value of the PKiKP/PcP amplitude ratio to evaluating its broad frequency characteristics, which is philosophically similar to how Cummins and Johnson (1988) evaluated pre-critical PKiKP waveforms and spectra by using a hybrid full wave-reflectivity algorithm. A dense configuration of borehole seismograms with high SNR observations of PKiKP waves over an unusually broad range of frequencies facilitates this new approach to estimate ICB properties. Thus, we examine data in the frequency domain and investigate possible broader implications for Earth's core dynamics.

Methods
Hi-net comprises approximately 700 short-period seismographs placed at the bottoms of individual boreholes (Okada et al. 2004). However, even for large-volume datasets such as Hi-net, good records of PKiKP and PcP are not frequently observed. We have detected PcP and PKiKP waveforms from 11 earthquakes with body wave magnitude ≥5.8 and focal depths of ≥80 km around Japan before the 2011 Tohoku earthquake (Fig. 2, Table 1). This covers epicentral distances from 15° to 50°. The reflection points of PKiKP at the ICB are distributed beneath the western Pacific, which is part of the eastern hemisphere (Fig. 2).

After visual examination of waveforms, amplitude spectra of PKIKP phases, and corresponding waveforms and spectra of pre-arrival noise, we applied a zero-phase Butterworth band-pass filter with corner frequencies of 2 and 5 Hz to 60 s record segments centered around theoretical PKiKP arrival times (Fig. 3a, b). This was

done for all records except the Mariana event (event 1), which was examined by Kawakatsu (2006) and observed to have large PKiKP signals around 1 Hz. Note that we use band-pass filtering only for initial identification of PKiKP.

After applying the band-pass filter described above and retrieving record segments of ±10 s length around PKiKP arrivals, seismograms were divided into subgroups comprising 70–230 stations with traces sorted by increasing epicentral distance. We then selected subsets of coherent waveforms by using the cross-correlation matrix method (Tkalčić et al. 2011), which retained 46–220 records per event. To find coherent PKiKP arrivals in each sub-group, we empirically determined the minimum percentage (τ) of all waveform pairs that should cross-correlate in such a way that the average cross-correlation coefficient equals or exceeds a threshold β. The algorithm calculates the cross-correlation coefficients for each pair of waveforms and counts the total percentage of pairs with cross-correlation coefficient exceeding β. For example, for $\beta > 0.4$, $\tau > 10\ \%$, and 130 total waveforms, we found that 77 waveforms satisfied these criteria and were consequently selected as "mutually coherent" (Fig. 3c). Incoherent waveforms were not used in further analyses. Subsequently, we visually checked the waveforms that satisfied the above criteria to find possible PKiKP signals with high signal-to-noise ratios, which resulted in a station list of "good" sites for PKiKP observations.

In the next step, we prepared a spectrogram of 90 s length from the unfiltered seismograms, with a sampling interval of 1 s and a lapse time of 50 s from the theoretical arrival times of PcP or PKiKP (Fig. 4). Each Fourier spectrum is calculated for a Welch tapered 10 s window (Press et al. 1988), then smoothed using a three-point moving average. Using the station list obtained with the
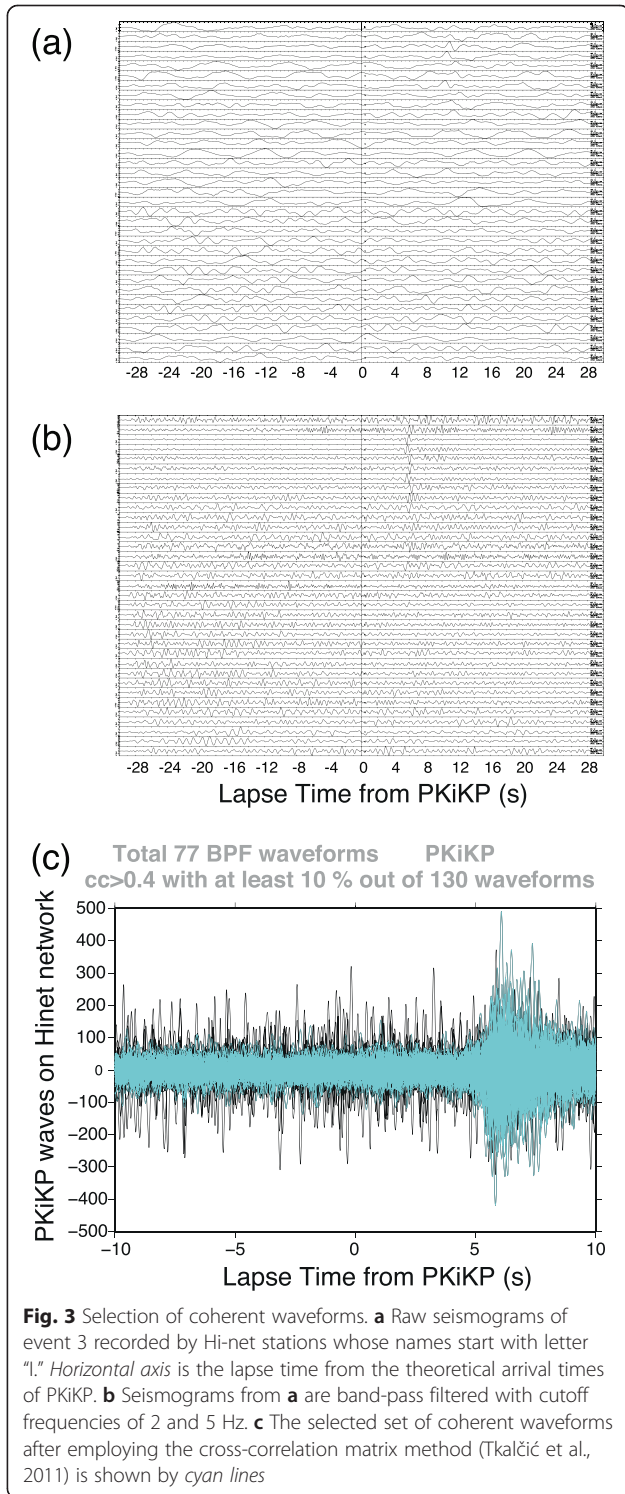
Fig. 3 Selection of coherent waveforms. **a** Raw seismograms of event 3 recorded by Hi-net stations whose names start with letter "I." *Horizontal axis* is the lapse time from the theoretical arrival times of PKiKP. **b** Seismograms from **a** are band-pass filtered with cutoff frequencies of 2 and 5 Hz. **c** The selected set of coherent waveforms after employing the cross-correlation matrix method (Tkalčić et al., 2011) is shown by *cyan lines*

cross-correlation matrix method, we used both the seismograms and spectrograms of PKiKP and PcP to identify acceptable data for calculating spectral ratios of PKiKP/PcP (Fig. 5). For each event, between 33 and 83 station records were retained (Table 1). Finally, the mean PKiKP/PcP spectral ratio was computed at each

frequency that exceeded the mean of the noise/PcP ratio (Fig. 5). The spectra of PcP and PKiKP contained several peaks and holes whose central frequencies were not uniform for all events. For example, for event 3, the spectral ratio of PKiKP/PcP exceeded the mean noise/PcP ratio in the range 0.8 to 3.0 Hz (Fig. 5a). In the case of other events, however, valid frequency ranges were somewhat different, e.g., 2–3 Hz for event 6 (Fig. 5b) and 1–4 Hz for event 11 (Fig. 5c). Despite the above restrictions, the relatively high-frequency content of the PcP and PKiKP waves means that these high-quality simultaneous observations over a broad frequency interval are unprecedented.

To correct the amplitude ratios, we determined focal mechanisms using the program of Kikuchi and Kanamori (2003), rather than cataloged Global CMT solutions, USGS Moment tensor, and double-couple solutions. The broadband displacements of P and SH waves in the frequency range 0.002–1 Hz were used for the inversion. Furthermore, we compared the short-period (SP) P wave amplitudes (1–5 Hz) with the radiation pattern predicted from each focal mechanism solution. Although the observed SP amplitudes showed a high degree of scatter, we found that some events had clear energy even near the nodal plane and null axis, suggesting a smoothed radiation pattern. This may be due to scattering near the source region, as discussed in previous studies that determined magnitudes from SP data (e.g., (Schweitzer and Kværna 1999; Takemura et al. 2015). These results are summarized in the Remarks column of Table 1. The smoothed radiation pattern for the short period is a likely explanation for the observation of PcP and PKiKP in the events from Kuril (event 2) and Mindanao (event 11), in which the take-off azimuths and angles of PcP and PKiKP were located near the nodal plane.

Attenuation factors for the mantle and core at arbitrary frequencies were normalized to a reference frequency of 1 Hz. We then obtained the corrected relationship between spectral and theoretical amplitude ratios from the following relationship:

$$
\left(\frac{A_{\mathrm{PKiKP}}}{A_{\mathrm{PcP}}}\right)_{\mathrm{corrected}} = \left(\frac{A_{\mathrm{PKiKP}}}{A_{\mathrm{PcP}}}\right)_{\mathrm{observed}} \frac{F_{\mathrm{PcP}}}{F_{\mathrm{PKiKP}}} \frac{\exp(-\pi f_0 \Delta t^*)}{\exp(-\pi f \Delta t^*)}
$$

$$
= \frac{T_{\mathrm{PK}} R_{\mathrm{KK}} T_{\mathrm{KP}}}{R_{\mathrm{PP}}} \frac{G_{\mathrm{PKiKP}}}{G_{\mathrm{PcP}}} \frac{\exp(-\pi f_0 t^*_{\mathrm{PKiKP}})}{\exp(-\pi f_0 t^*_{\mathrm{PcP}})},
$$

(1)

where the subscripts PKiKP and PcP denote the corresponding seismic phases. On the left side of the equation, A is the spectral amplitude at an arbitrary frequency, F is the focal mechanism radiation pattern, t^* is the anelastic parameter (Lay and Wallace 1995), and Δt^* is the differential anelastic parameter between PKiKP